

Fully Integrated Passive UHF RFID Transponder IC With $16.7\text{-}\mu\text{W}$ Minimum RF Input Power

Udo Karthaus, *Member, IEEE*, and Martin Fischer

Abstract—This paper presents a novel fully integrated passive transponder IC with 4.5- or 9.25-m reading distance at 500-mW ERP or 4-W EIRP base-station transmit power, respectively, operating in the 868/915-MHz ISM band with an antenna gain less than -0.5 dB. Apart from the printed antenna, there are no external components. The IC is implemented in a $0.5\text{-}\mu\text{m}$ digital two-poly two-metal digital CMOS technology with EEPROM and Schottky diodes. The IC's power supply is taken from the energy of the received RF electromagnetic field with help of a Schottky diode voltage multiplier. The IC includes dc power supply generation, phase shift keying backscatter modulator, pulse width modulation demodulator, EEPROM, and logic circuitry including some finite state machines handling the protocol used for wireless write and read access to the IC's EEPROM and for the anticollision procedure. The IC outperforms other reported radio-frequency identification ICs by a factor of three in terms of required receive power level for a given base-station transmit power and tag antenna gain.

Index Terms—Passive transponder, radio-frequency identification (RFID), low-power low-voltage CMOS, backscatter modulation.

I. INTRODUCTION

THE AREA OF applications for radio-frequency identification (RFID) is increasing rapidly. Applications include supply chain management, access control to buildings, public transportation, and open-air events, airport baggage, express parcel logistics, and many more. The need for high volume, low cost, small size and large data rate is increasing, while stringent regulations of transmit power and bandwidth have to be met. The IC presented in this paper fulfills all these stringent requirements.

Traditionally, passive transponders operate at 125 kHz or 13 MHz using coils as antennas. These transponders operate in the magnetic near field of the base station's coil antenna, and their reading distance is typically limited to less than 1.2 m, e.g., 22 cm with a $9\text{-cm} \times 19\text{-cm}$ antenna [1], and bandwidth in Europe and other regions is limited by regulations to a few kilohertz. A problem of these systems is the low efficiency of reasonably sized antennas at such low frequencies. Due to great demand for higher data rates, longer reading distances, and small antenna sizes, there is a strong interest in UHF frequency band RFID transponders, especially for the 868/915-MHz and 2.4-GHz ISM bands. However, all UHF transponders

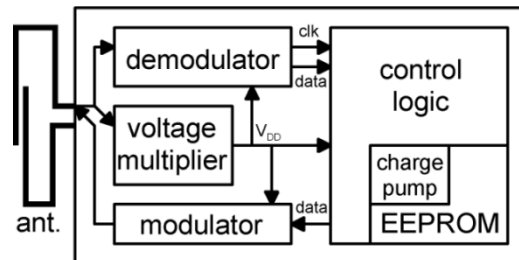


Fig. 1. Architecture of the transponder IC.

commercially available today need to have about $150\text{-}\mu\text{W}$ input power which leads to a reading distance of about 2 m (antenna gain about 0 dB and 500-mW ERP) [2]. Recently, a new product with $60\text{-}\mu\text{W}$ peak RF input power has been announced which leads to a reading distance of about 3.3 m (antenna gain about 0 dB and 500-mW ERP when an average input power of $54\text{ }\mu\text{W}$ is assumed) [3]. In Europe, regulations currently limit base-station transmit power to 500-mW ERP in the 868-MHz ISM band and bandwidth to 250 kHz.

The goal of this project was to design a transponder with increased reading distance by using a different voltage generator topology and by employing a very well-suited technology. The technology is a two-metal two-poly $0.5\text{-}\mu\text{m}$ digital CMOS process supporting EEPROM and Schottky diodes. Advanced low-voltage low-power circuit design techniques have been employed. Careful design of the protocol, the control logic, and the EEPROM allows to operate the IC with only $1.5\text{ }\mu\text{A}$ at 1.5-V supply voltage in all modes except writing to the EEPROM where $2.5\text{ }\mu\text{A}$ are needed. The specially designed Schottky diodes with low series resistance allow for a high-efficiency conversion of the received RF input signal energy to dc supply voltage. The EEPROM is used for random wireless write and read access to the tag.

Sections II and III describe the system architecture and the operation of the different building blocks, respectively. In Section IV, optimization problems and analyses like the optimum type of modulation and influence of Schottky diode parasitics are discussed in more detail. In Section V, the experimental results are presented, and a summary and conclusions are provided in Section VI.

II. ARCHITECTURE

Fig. 1 shows a block diagram of the IC. The individual blocks of this diagram are described in more detail in the following paragraphs. The antenna is the only external component of the transponder. In the example shown in Fig. 8, a printed modified loop antenna is used. It provides low loss and is power matched to the average input impedance of the voltage multiplier. The

Manuscript received January 21, 2003; revised June 26, 2003. This work was supported in part by the European Commission under Grant IST IST1999-10339, s. [4].

U. Karthaus is with the ATMEL Germany GmbH, D-89081 Ulm, Germany (e-mail: udo.karthaus@hno.atmel.com).

M. Fischer is with the ATMEL Germany GmbH, D-74072 Heilbronn, Germany (e-mail: martin.fischer@hno.atmel.com).

Digital Object Identifier 10.1109/JSSC.2003.817249

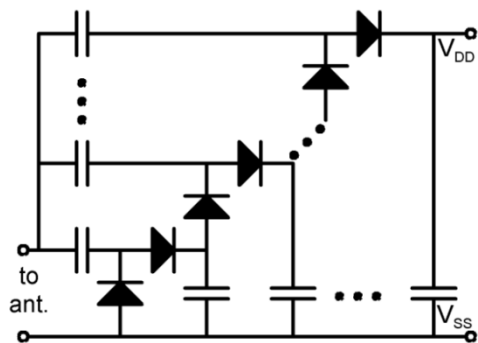


Fig. 2. Schematic of the voltage multiplier converting the RF input signal to dc supply voltage.

voltage multiplier converts a part of the incoming RF signal power to dc for power supply for all active circuits on the chip. A 250-pF blocking capacitor stores supply energy during short gaps in the received signal of up to approximately 100 μ s (0.6-V voltage drop at 1.5- μ A supply current). The demodulator converts the pulse-width modulated input signal to digital data and generates a synchronous system clock. The data can be write, read, or anticollision commands, as well as data to be written to the EEPROM. The modulator converts data from the control logic to changes in the input impedance using a MOS varactor. This data can be acknowledgment of received commands or data read from the EEPROM. The logic circuitry handles the protocol, including anticollision features, cyclic redundancy checks (CRC) checks, error handling, enabling and disabling of analog circuits (power down, standby, power up), etc. Further details of logic circuitry and protocol issues are beyond the scope of this paper.

A charge-pump circuit converts the dc supply voltage of 1.5–2.5 V to a voltage of approximately 14 V needed for programming the EEPROM. The charge pump utilizes the same Schottky diodes and almost the same architecture as the voltage multiplier used for dc power supply generation. It works at a frequency of approximately 300 kHz generated by an on-chip RC-type oscillator.

III. BUILDING BLOCKS

A. DC Supply Voltage Generation

The dc power supply is generated from the incident RF signal power by the voltage multiplier circuit shown in Fig. 2, sometimes also called “charge pump” in the context of memory ICs. The diodes are Silicon–Titanium Schottky diodes with low series resistance of $<300\ \Omega$ and low Schottky junction capacitance of approximately 12 fF. For the RF signal, all the diodes are connected in parallel (or antiparallel) by the poly–poly capacitors. For dc, however, they are connected in series to allow a dc current flowing between V_{DD} and V_{SS} terminals. The voltage generated between these nodes is approximately equal to

$$V_{DD} = n \cdot (V_{p,RF} - V_{f,D}) \quad (1)$$

where n is the number of diodes, $V_{p,RF}$ is the amplitude of the RF input signal, and $V_{f,D}$ is the forward voltage of the Schottky diodes, which is approximately 200 mV at 7 μ A.

The input impedance is mainly determined by the junction and substrate capacitances of the Schottky diodes. The real part

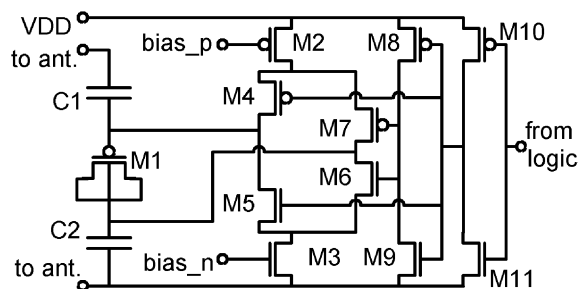


Fig. 3. Schematic of the backscatter phase modulator.

of the impedance is much lower than the imaginary part and is strongly dependant on the dc current taken from the V_{DD} output. For a typical operating point of $V_{DD} = 1.5$ V and $I_{DD} = 1.5\ \mu$ A, the real part of the impedance is approximately 30 times lower than the imaginary (capacitive) part. In other words, the IC’s input capacitance has a quality factor Q of 30. This places high demands on the antenna, which needs to be matched to the IC’s input impedance for sufficiently good power efficiency. Such high quality factors of the IC’s input impedance can only be achieved by minimizing power loss in all parts of the circuit. This requires very careful layout with low series resistance and substrate capacitances of the on-chip interconnect lines as well as high- Q Schottky diodes and poly–poly capacitors. The latter are realized with a high aspect ratio and metal over the top poly plate and along both sides of the bottom poly plate to reduce the series resistance.

B. Modulator

The modulation is done using a backscatter approach. When the backward link is active, the base station transmits a continuous-wave (CW) carrier with some small notches for the data transfer. By changing the IC’s input impedance, the electromagnetic wave scattered back by the antenna is modulated. This modulated backscattered signal is used for the reverse link from IC to base station. The modulator shown in Fig. 3 changes the input capacitance (rather than the input resistance), leading to a phase modulation [phase shift keying (PSK), rather than amplitude shift keying (ASK)] of the backscattered wave. The input impedance is changed with help of accumulation mode MOS varactor M1. With help of the two poly–poly capacitors C1 and C2, the dc voltage across the varactor can be set to plus or minus V_{DD} , thereby changing the varactor’s capacitance between its maximum and minimum value. M8 to M11 operate as two simple inverters for the incoming logic signal. Depending on the logic state, either M4 and M6 or M5 and M7 are switched off. Biasing of M2 and M3 decides how fast the varactor is discharged and recharged, thereby determining the bandwidth of the backscattered signal to be consistent with regulations. The g_{d0} of M2 and M3, which operate in triode region most of the time, is designed to be $<10\ \mu$ S in order not to cause significant RF power loss.

With this PSK approach, high power efficiency for dc voltage generation and high modulated backscattered power for the reverse link are achieved simultaneously. Formulas for both modulation and power efficiency and for different modulation types are given in Section IV. Furthermore, the signal-to-noise ratio

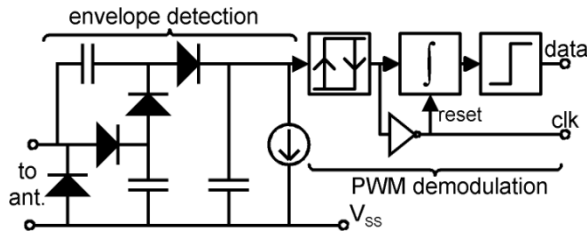


Fig. 4. Functional block diagram of the demodulator.

(SNR) and the bit-error rate (BER) are better than when using ASK.

C. Demodulator

For the forward link from base station to transponder, a pulse-width modulation (PWM) scheme is used. The gaps between pulses are approximately $4\text{-}\mu\text{s}$ long; short enough to allow a continuous power supply of the transponder, but long enough to comply with the stringent bandwidth regulations in Europe and elsewhere. The transponder uses an envelope detector and a pulse-width demodulator for demodulation, as shown in Fig. 4. The envelope detection uses the same voltage multiplier circuit topology than the dc voltage supply generation, but with four diodes instead of ten and smaller poly-poly capacitors. These capacitors together with the current sink determine the minimum width of gaps that can be detected by the circuit. The inverted output signal is used as a “system clock” for the FSM and for the internal clock generation center, where each rising edge denotes the arrival of a new bit. This signal is also used to reset the integrator which measures the duration of each pulse. A simple discriminator decides whether a pulse is “long” or “short.”

IV. OPTIMIZATION ANALYSIS

A. Supply Voltage Generation

A voltage multiplier converting the RF input signal to dc supply voltage is shown in Fig. 2. The design parameters of the voltage multiplier are a tradeoff between power efficiency, useful impedance, and operating point (load). Optimization parameters include the number of stages, the size of Schottky diodes, and the size of coupling capacitors.

To get a good efficiency, it is very important to have Schottky diodes with large saturation current I_s (resulting in low forward voltage drop) and a low junction capacitance C_j , as well as a small series resistance R_s and small parasitic capacitance C_{sub} to substrate. Larger Schottky diodes have a larger saturation current I_s and a smaller series resistance R_s , but also larger junction and substrate capacitances, which then may dominate the power losses, so that an optimum size of the Schottky diode has to be found.

Similarly, for the coupling capacitors in Fig. 2 it is also important to have small R_s and C_{sub} . However, C_{sub} is proportional to the wanted capacitance C (both capacitances are proportional to the area). Since a certain amount of coupling is needed, C and C_{sub} cannot be made arbitrarily small. R_s can be minimized using a large aspect ratio or multifinger capacitors.

Power losses due to substrate capacitances of diodes, interconnect lines, or capacitors can be determined and optimized using the following equation:

$$P_{\text{loss}} = \frac{1}{2}v^2 \frac{R_{\text{sub}}}{R_{\text{sub}}^2 + (\omega C_{\text{sub}})^{-2}} \approx \frac{1}{2}v^2(\omega C_{\text{sub}})^2 R_{\text{sub}} \quad (2)$$

where v is the device’s RF peak voltage with respect to substrate, C_{sub} is the capacitance to substrate, R_{sub} is the series resistance of C_{sub} , and ω is the angular frequency of the input signal. The approximation is valid if $R_{\text{sub}}\omega C_{\text{sub}} \ll 1$, which is usually true for low-resistivity substrates of digital CMOS technologies. From (2) it can be seen that there is a quadratic dependency of substrate loss on capacitance as well as on frequency, which explains the much lower power efficiency of the front-end at 2.45 GHz compared with 868 or 915 MHz.

B. Modulator: Power Efficiency and Backscattered Modulated Power

Modulation of the backscattered wave is achieved by changing the IC’s input impedance between two different states, $Z_1 = R_1 + jX_1$ and $Z_2 = R_2 + jX_2$. This section discusses whether it is more advantageous to modulate the real part or the imaginary part of the impedance, and by how much it should be modulated. Two things need to be taken into account in this analysis: the RF power available for dc supply power generation and the modulated backscattered power of the reverse link, from transponder to base station. First, the equations for RF input power to the voltage multiplier and for backscattered modulated power are derived. Afterwards, these equations are applied to the cases of ASK and PSK.

1) *Power Supply Efficiency:* The RF input power available to the voltage multiplier for dc power generation for the two impedance states 1 and 2 is given by

$$\begin{aligned} P_{\text{RF,in,1,2}} &= \frac{1}{2}\text{Re}(v_{\text{in}}^* \cdot i_{\text{in}}) \\ &= \frac{1}{2}\text{Re} \left(\frac{v_0^2(R_{1,2} - jX_{1,2})}{|R_{1,2} + R_{\text{ant}} + j(X_{1,2} + X_{\text{ant}})|^2} \right) \\ &= \frac{1}{2} \frac{v_0^2 \cdot R_{1,2}}{(R_{1,2} + R_{\text{ant}})^2 + (X_{1,2} + X_{\text{ant}})^2} \\ &= \underbrace{\frac{v_0^2}{8R_{\text{ant}}}}_{\text{available power}} \cdot \left(1 - \underbrace{\frac{|Z_{1,2} - Z_{\text{ant}}^*|^2}{|Z_{1,2} + Z_{\text{ant}}|^2}}_{\text{ratio of power reflected}} \right) \end{aligned} \quad (3)$$

where v_{in} is the peak voltage at the IC’s input, i_{in} is the peak current flowing between antenna and IC, and v_0 is the peak source voltage that would be observed if the antenna were not loaded by the IC. With the power available from the antenna being

$$P_{\text{avail}} = \frac{v_0^2}{8R_{\text{ant}}} \quad (4)$$

and the reflection coefficients defined as

$$\rho_{1,2} = \frac{Z_{1,2} - Z_{\text{ant}}^*}{Z_{1,2} + Z_{\text{ant}}} \quad (5)$$

(3) simplifies to

$$P_{\text{RF},\text{in},1,2} = P_{\text{avail}}(1 - |\rho_{1,2}|^2). \quad (6)$$

For optimum power supply efficiency, power matching between antenna and IC for both states would be optimum: $Z_1 = Z_2 = Z_{\text{ant}}^*$, where $Z_{\text{ant}}^* = R_{\text{ant}} - jX_{\text{ant}}$ is the complex conjugate of the antenna impedance. In this case, all the available power would be available to the rectifier:

$$P_{\text{RF},\text{in},1} = P_{\text{RF},\text{in},2} = P_{\text{avail}}. \quad (7)$$

Obviously, this conflicts with the need for two *different* impedances for modulation. Therefore, both power supply efficiency and modulation efficiency need to be taken into account for optimization of the modulator.

If the IC is in state 1 and 2 for a fraction of p_1 and p_2 of time, respectively, the average input power available for the power supply is

$$\begin{aligned} P_{\text{RF},\text{in}} &= p_1 P_{\text{RF},\text{in},1} + p_2 P_{\text{RF},\text{in},2} \\ &= P_{\text{avail}}(p_1(1 - |\rho_1|^2) + p_2(1 - |\rho_2|^2)). \end{aligned} \quad (8)$$

2) *Modulation Efficiency*: The antenna impedance can be rewritten as

$$Z_{\text{ant}} = R_{\text{rad}} + R_{\text{loss}} + jX_{\text{ant}} \quad (9)$$

where R_{loss} accounts for ohmic and dielectric losses in the antenna and R_{rad} is the radiation resistance of the antenna. The antenna loss factor is

$$L_{\text{ant}} = \frac{R_{\text{rad}} + R_{\text{loss}}}{R_{\text{rad}}} = \frac{R_{\text{ant}}}{R_{\text{rad}}}. \quad (10)$$

Assuming that both states are active an equal amount of time, $p_1 = p_2 = 0.5$, the modulated backscattered power is found to be

$$P_{\text{bs}} = \frac{|i_2 - i_1|^2}{8} R_{\text{rad}} \quad (11)$$

where $i_{1,2}$ are the complex amplitudes of the current flowing between antenna and IC for the two states 1 and 2. With

$$\begin{aligned} i_{1,2} &= \frac{v_0}{Z_{\text{ant}} + Z_{1,2}} \\ &= \frac{v_0}{2R_{\text{ant}}}(1 - \rho_{1,2}) \end{aligned} \quad (12)$$

(11) can also be expressed in terms of reflection coefficients:

$$\begin{aligned} P_{\text{bs}} &= \frac{v_0^2 R_{\text{rad}}}{32R_{\text{ant}}^2} |(1 - \rho_2) - (1 - \rho_1)|^2 \\ &= \frac{P_{\text{avail}}}{4L_{\text{ant}}} |\rho_1 - \rho_2|^2. \end{aligned} \quad (13)$$

This is the total power of the two sidebands of the backscattered wave, excluding the carrier power. In the following, three types of modulation are compared:

- 1) ASK with power match in one of the two states and total reflection (short or open) in the other state;
- 2) PSK with an equal amount of mismatch in both states;
- 3) ASK with an equal amount of mismatch in both states.

The distinction between amplitude and phase shift keying refers to the currents i_1 and i_2 . For ASK, the amplitude of the

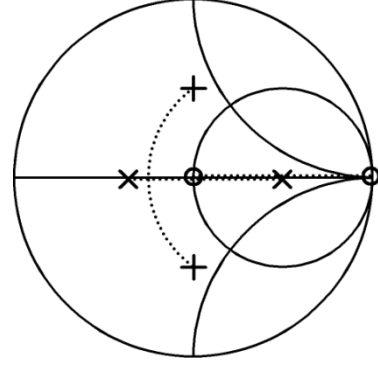


Fig. 5. Three different modulation types visualized for the case $m = 0.5$ in a Smith chart. “O”: ASK with total mismatch in one state, case 1); “+”: PSK, case 2); “X”: ASK with equal mismatch in both states, case 3).

current is modulated. This is achieved by a change in the real part of the impedance and of the reflection coefficient. For PSK, the phase of the current is modulated, which is achieved by a change in the imaginary part of the input impedance and of the reflection coefficient.

a) *ASK With Total Mismatch in One State*: This type of modulation is widely used, especially in typical 13-MHz and 125-kHz inductive systems. The antenna is disconnected or shorted in one state, $Z_1 = 0$ or $Z_1 = \infty$, $|\rho_1| = 1$, and matched to the antenna impedance in the other state, $Z_2 = A_{\text{ant}}^*$, $|\rho_2| = 0$. This is also shown in the Smith chart of Fig. 5 by the circles for the case of disconnecting the antenna in state 1. Reflection coefficients read from the Smith chart are according to the definition in (5). Impedances read from this Smith chart are the IC’s input impedance plus the imaginary part of the antenna impedance, $Z_{1,2} + jX_{\text{ant}}$, normalized by the real part of the antenna impedance, R_{ant} . According to (11) or (13)

$$P_{\text{bs,ask,on-off}} = \frac{P_{\text{avail}}}{4L_{\text{ant}}} \quad (14)$$

assuming $p_1 = p_2 = 0.5$. Only in state 2 is all the available power available to the voltage multiplier, whereas in state 1 all power is reflected. So the average RF input power available to the IC equals

$$P_{\text{RF},\text{in,ask,on-off}} = p_1 P_{\text{avail}}. \quad (15)$$

In modulation schemes, where one of the two states is active most of the time, e.g., $p_2 \ll p_1 \approx 1$, this is a good choice in terms of power efficiency, but these schemes require a much larger bandwidth (due to the short gaps) which is often prohibited by national authorities’ regulations. Also, the backscattered modulated power is smaller than in (14) which only holds for $p_1 = p_2 = 0.5$. In the case $p_1 = p_2 = 0.5$, assuming there are no antenna losses, i.e., $L_{\text{ant}} = 1$, 50% of the available input power is actually available for rectification, 25% is used as backscattered modulated power, and the remaining 25% is wasted. This is indicated by the filled circle at $m = 0.5$ in Fig. 6.

b) *PSK*: PSK is used by the IC presented in this paper. The real part of the reflection coefficient is ideally zero for both states, and the imaginary part equal in magnitude and opposite in sign: $\rho_{1,2} = \pm jm$, where $0 < m < 1$ is the modulation index.

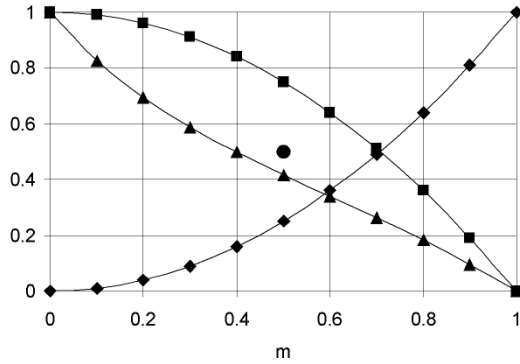


Fig. 6. Power efficiency for different modulation types versus modulation index m . Diamonds: Backscattered modulated power (valid for all modulation types). Squares, triangles, and circles: RF power available to the rectifier. Squares: PSK, case 2); triangles: ASK with equal mismatch in both states, case 3); circles: ASK with total mismatch in one state, case 1). (All power values relative to the available input power assuming a lossless antenna).

In this case, from (13) and (6) the modulated backscattered power and the rectifier RF input power are found to be

$$P_{bs,psk} = m^2 \frac{P_{avail}}{L_{ant}} \quad (16)$$

and

$$P_{RF,in,psk,1} = P_{RF,in,psk,2} = (1 - m^2)P_{avail} \quad (17)$$

respectively.

Assuming again the lossless case $L_{ant} = 1$, we see that in contrast to case 1), PSK uses all available power either for the rectifier or for modulation, since the sum of (16) and (17) equals the total available power P_{avail} .

In the special case of our application, where the change in imaginary part of impedance is approximately equal to the real part of the impedance, corresponding to $m = \sqrt{2} - 1 \approx 0.41$, the backscattered power and the RF input power are equal to

$$P_{bs,psk}|_{m=\sqrt{2}-1} = (3 - 2\sqrt{2}) \frac{P_{avail}}{L_{ant}} \approx 0.17 \frac{P_{avail}}{L_{ant}} \quad (18)$$

and

$$P_{RF,in,psk}|_{m=\sqrt{2}-1} = 2(\sqrt{2} - 1)P_{avail} \approx 0.83P_{avail} \quad (19)$$

respectively. These percentages can also be read from the two curves marked with diamonds ($P_{bs,psk}$) and squares ($P_{RF,in,psk}$) in Fig. 6. The change in reflection coefficient between the two states is shown in the Smith chart of Fig. 5 by the “+” signs.

c) *ASK With Finite Mismatch in Both States:* A third possible type of modulation is changing the real part of the reflection coefficient like in case 1), but with the amount of mismatch being equal in both states, $\rho_{1,2} = \pm m$, where m is again a modulation index.

Just like for PSK, from (13) and (8) we find

$$P_{bs,ask} = m^2 \frac{P_{avail}}{4L_{ant}} \quad (20)$$

and

$$P_{RF,in,ask,1} = P_{RF,in,ask,2} = (1 - m^2)P_{avail}. \quad (21)$$

This kind of modulation can most easily be achieved by switching a resistor in series or in parallel to IC's input in one of the two states. The power lost in this resistor is the main disadvantage compared with PSK modulation. The following derivations are not valid for any other possible kinds of achieving ASK modulation that might waste less input power. To calculate this power, we need to know the impedances in both states.

Solving (5) for $Z_{1,2}$ yields

$$\begin{aligned} Z_{1,2} &= -Z_{ant} + \frac{2R_{ant}}{1 - \rho_{1,2}} \\ &= -jX_{ant} + \frac{1 + \rho_{1,2}}{1 - \rho_{1,2}} R_{ant}. \end{aligned} \quad (22)$$

With $\rho_{1,2} = \pm m$, we get

$$Z_{1,2} = -jX_{ant} + \frac{1 \pm m}{1 \mp m} R_{ant}. \quad (23)$$

Assuming a series resistor is used in state 2, the value of this series resistor is

$$\begin{aligned} R_{series} &= R_2 - R_1 \\ &= \left(\frac{1 \pm m}{1 \mp m} - \frac{1 \pm m}{1 \mp m} \right) R_{ant} \\ &= \frac{4m}{1 - m^2}. \end{aligned} \quad (24)$$

The fraction of the total IC input power, which is not wasted by the series resistor, but actually available to the rectifier during state 2, equals

$$\begin{aligned} \frac{R_2 - R_{series}}{R_2} &= \frac{R_1}{R_2} \\ &= \frac{1 - m}{1 + m} \frac{R_{ant}}{R_{ant}} \\ &= \frac{1 - m}{1 + m} \frac{R_{ant}}{R_{ant}} \\ &= \left(\frac{1 - m}{1 + m} \right)^2. \end{aligned} \quad (25)$$

The time-averaged usable input power is therefore

$$\begin{aligned} P_{RF,in,ask} &= \frac{1}{2}(1 - m^2)P_{avail} \\ &\quad + \frac{1}{2}(1 - m^2) \left(\frac{1 - m}{1 + m} \right)^2 P_{avail} \\ &= \frac{1 - m^4}{(m + 1)^2} P_{avail}. \end{aligned} \quad (26)$$

If the same amount of backscattered power is needed as in the example in case 2), where $m = \sqrt{2} - 1$, according to (25) approximately 83% of the input power is wasted by the series resistor during state 2.

Fig. 6 shows the modulated backscattered power and the voltage multiplier input power versus modulation index m for both, PSK and ASK with finite, equal mismatch in both states. The curve marked with triangles shows the modulated backscattered power normalized by the total available power and is valid for ASK and PSK. Power available to the rectifier is marked with squares (PSK), triangles (ASK with equal mismatch for both states). It can be seen that only for very small modulation index m , ASK efficiency is almost comparable to

TABLE I
ON-WAFER MEASUREMENT RESULTS OF THE VOLTAGE MULTIPLIER

Test conditions	$\text{Re}(Z_{1,2})$ [Ω]	$\text{Im}(Z_{1,2})$ [Ω]	Vdc [V]	Idc [μA]	Efficiency [%]	RF input power [μW]
869 MHz, idle	5.7 / 4.5	-218 / 203	1.5	0.95	14.5	9.8
869 MHz, active	6.7 / 5.5	-218 / 203	1.5	1.5	18	12.5
2.45 GHz, active	4.0 / 3.8	-89 / -84	1.5	1.5	5	45

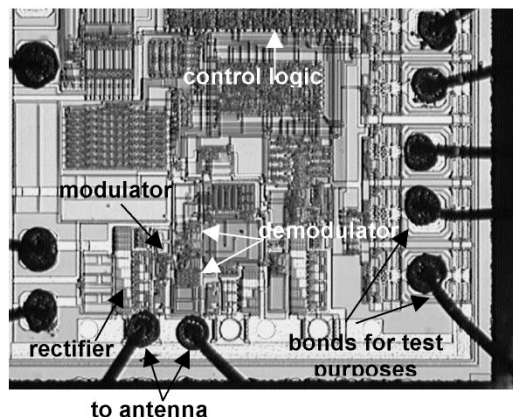


Fig. 7. Die photograph.

PSK. For greater m , a large portion of power is wasted in the modulation resistor. The above calculations do not include the effect that the efficiency of the rectifier is lower for state 2 than for state 1, because the net input power is lower. This increases the difference between ASK and PSK in terms of power efficiency even a little further. Case 1) is also indicated in Fig. 6 by the filled circle at $m = 0.5$. Comparing the three modulation types at $m = 0.5$, where the backscattered modulated power is equal for all three cases, we get an RF input power to the rectifier of 42%, 50%, and 75% for the three cases 1), 3), and 2), respectively.

V. EXPERIMENTAL RESULTS

A die photograph is shown in Fig. 7. The different sub-circuits, such as rectifier, modulator, demodulator, and control logic, are labeled. In the typical application, only two bond wires are needed to connect the antenna to the IC. The other bonds seen in Fig. 7 are used for experimental test purposes. The die photograph only shows the analog circuitry and a small part of the logic control circuits. The upper part not shown contains the EEPROM and the rest of the logic circuitry. Fig. 8 shows an assembled prototype transponder tag including the printed modified loop antenna. More compact antenna designs are possible. Especially if the IC is used in the 2.45-GHz ISM band, which is possible without any changes to the IC, the antenna would be much smaller.

Measurements concerning the efficiency of the voltage multiplier and the input impedance of the transponder have been made and compared with simulations. Measurement results and simulations agree very well within normal process tolerances and measurement tolerances. Table I shows the input impedance for both modulator states $Z_{1,2}$ and the efficiency of the 869-MHz transponder and the 2.45-GHz transponder.

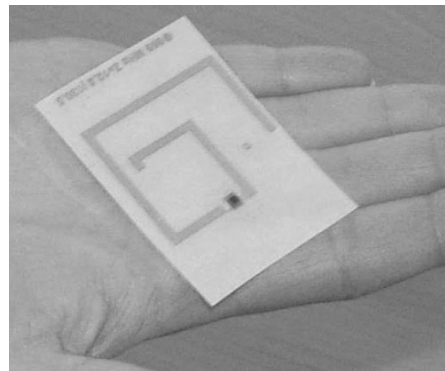


Fig. 8. Photograph of an assembled transponder tag.

If there is no communication between base station and transponder (idle running), the 869-MHz transponder needs only $0.95 \mu\text{A}$ and the efficiency of the voltage multiplier is 14.5%. If there is a communication (e.g., reading the transponder), the current consumption and power efficiency increase to $1.5 \mu\text{A}$ and 18%, respectively. The dependence of current on efficiency can be seen by looking at Fig. 9. The higher the current, the better is the efficiency. Therefore, decreasing the current by a factor of two does not decrease the needed power by a factor of two. Also, the real part of the transponder impedance increases slightly with higher current while the imaginary part stays constant.

The experimental results achieved with the setup of Fig. 8 and with on-wafer measurements are as follows.

Successful communication between a base station operating at 869 MHz and 500-mW ERP and a transponder as shown in Fig. 8 has been achieved in an anechoic chamber over a distance of 4.5 m. Considering free space propagation “loss” and assuming a 0-dB transponder antenna gain, this corresponds to an RF input power of $30 \mu\text{W}$. The actual RF input power was somewhat lower than $30 \mu\text{W}$ due to an antenna gain below -0.5 dB and due to unavoidable mismatch caused by the modulation of the input impedance during communication. In the U.S., where 4-W EIRP is allowed at 915 MHz, an RF input power of $30\text{-}\mu\text{W}$ corresponds to a reading distance of 9.25 m.

With on-wafer measurements, where antenna loss is not present and mismatch can be measured and eliminated, the actual input power needed was found to be only $12.5 \mu\text{W}$ in read mode and $35 \mu\text{W}$ during write access to the EEPROM. Taking into account the unavoidable mismatch introduced by modulation with an modulation index of $m = 0.5$, the minimum available input power according to (17) is $16.7 \mu\text{W}$. According to (16), the whole difference of $4.2 \mu\text{W}$ (25%) is utilized as backscattered modulated power. The difference of the values of $30 \mu\text{W}$ obtained in the anechoic chamber and $16.7 \mu\text{W}$ from the on-wafer measurements is greater than the

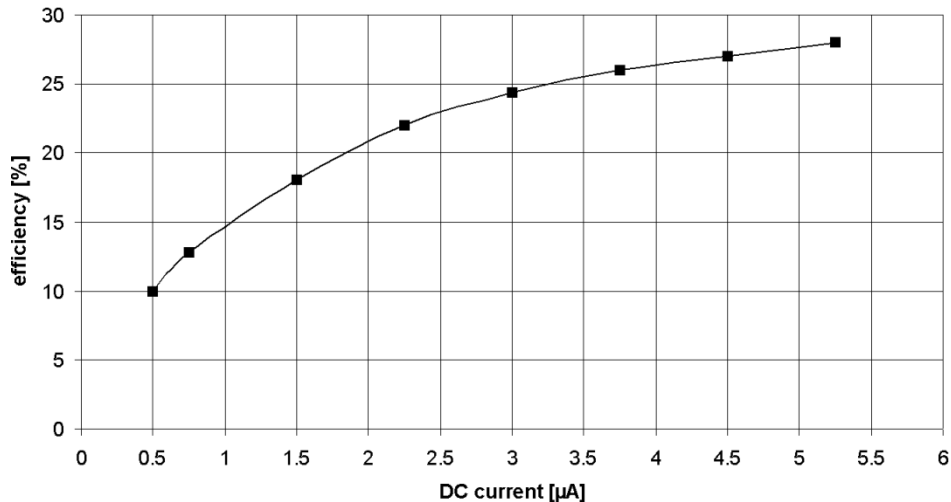


Fig. 9. Efficiency versus dc current.

−0.5-dB maximum antenna gain. Possible reasons for this are additional impedance mismatch due to nonoptimal antenna impedance (real and/or imaginary part) and an antenna orientation with lower antenna gain than the maximum measured gain of −0.5 dB.

Also the results for a transponder designed for 2.45 GHz are shown in Table I. The imaginary part of the input impedance is lower because the frequency is higher. The efficiency is much smaller (5%) because all parasitic substrate capacitances have a larger influence and generate much more losses, as can be seen from (2).

On-wafer measurements showed that the RF input power for read and write access to the transponder is 50 and 126 μW , respectively. With 4-W EIRP at 2.45 GHz and 0-dB transponder antenna gain, and assuming that 25% of the available input power are reflected due to modulation mismatch, this corresponds to a reading distance of 2.6 m and a programming distance of 1.1 m, respectively.

VI. CONCLUSION

This paper presents a novel passive UHF transponder. Theoretical analyses used for the design optimization have been presented. By using a 0.5- μm CMOS technology with EEPROM and Schottky diodes, a new voltage generation topology, PSK in backward link, and careful layout and antenna matching, a free space reading distance of 4.5 m was achieved with only 500-mW ERP base-station transmit power. At this distance, the received power level at the IC's input is 16.7 μW , whereof the available dc power is approximately 2.25 μW (1.5 μA , 1.5 V, and 18% rectifier efficiency) and the modulated backscattered power is approximately 4.2 μW (25%). In the U.S., where 4-W EIRP transmit power is allowed, the reading distance would be approximately 9.25 m. This is a huge improvement compared with any UHF transponder reported in scientific journals or conferences, showing reading distances below 1.5 m, and still a significant improvement compared with [3].

ACKNOWLEDGMENT

The authors would like to thank O. Jakkola, T. Varpula, and H. Seppä of VTT, Finland, for antenna design and measurements,

U. Friedrich and D. Ziebertz of Atmel Germany for design of low-power control logic and of the protocol, V. Flassnöcker of Atmel Germany for designing the charge pump for the EEPROM, and S. Furic and P. Crevel of Atmel Nantes for designing and modeling the Schottky diodes and MOS varactors.

REFERENCES

- [1] R. M. Hornby, "RFID solutions for the express parcel and airline baggage industry," in *Proc. IEE Colloq. RFID Technology*, London, U.K., Oct. 1999, pp. 2/1–2/5.
- [2] K. V. S. Rao, "An overview of backscattered radio frequency identification system (RFID)," in *Proc. Asia Pacific Microwave Conf.*, vol. 3, Singapore, Dec. 1999, pp. 746–749.
- [3] CID ISO18000-6B presentation, Phillips Semiconductor, Cedar Rapids, IA, 2002.
- [4] The Palomar Project, "Passive Long Distance Multiple Access UHF RFID System," European Commission, Public Report, Project Number IST1999-10339, Nov. 2002.



Udo Karthaus (S'99-M'02) received the Dipl.-Ing. and Dr.-Ing. degrees in electrical engineering at the University of Paderborn, Paderborn, Germany in 1995 and 2000, respectively.

From 1995 to 2000 he was a Research Assistant at the "Optical Communications and High Frequency Engineering" Lab. at the University of Paderborn. He worked on measurement and simulation of broadband, time-varying 30–60 GHz communication channels. From 2000 to 2001 he worked on the design of passive transponder ICs for the automotive division of Atmel in Heilbronn, Germany. Since July 2001, he has been with the RF communications division of Atmel in Ulm, Germany.

Dr. Karthaus received the NORTEL best paper award at the International Symposium on Communications Systems and Digital Signal Processing (CSDSP), Sheffield, U.K., Apr. 6–8, 1998.



Martin Fischer was born in Schwäbisch Hall, Germany, in 1973. He received the Dipl.-Ing. (FH) degree in electronic engineering from Fachhochschule Heilbronn, Heilbronn, Germany in 2000.

In 2000 he joined Atmel Germany, Heilbronn where he is working in the RFID group within the automotive division. His technical interests are in the field of very low-power analog CMOS circuits and RF IC design.